

# Analysis the Influence of Various Step Punch Shape and Clearance in Stretch Flanging Process Using FEM Simulation

Surendra Kumar<sup>1\*</sup>, Manoj Soni<sup>2,3,4\*</sup>, S.K. Panthi<sup>3</sup>, M. Ahmed<sup>3</sup> and Yogesh Dewang<sup>5</sup>

<sup>1</sup>Motherson Technology Services Limited, Bangalore, Karnataka, India

<sup>2</sup>AcSIR, Ghaziabad, Uttar Pradesh, India

<sup>3</sup>CSIR- AMPRI, Bhopal, Madhya Pradesh, India

<sup>4</sup>Bansal institute of science and technology (BIST) Bhopal, Madhya Pradesh, India

<sup>5</sup>Lakshmi Narain College of Technology (LNCT), Bhopal, Madhya Pradesh, India

## \*Correspondence to:

Surendra Kumar

Motherson Technology Services Limited,  
Bangalore, Karnataka, India.

E-mail: [surendra.javapatel@gmail.com](mailto:surendra.javapatel@gmail.com)

Manoj Soni

AcSIR, Ghaziabad, India.

CSIR-AMPRI, Bhopal, India.

Bansal institute of science and technology  
(BIST), Bhopal, India.

E-mail: [soni44@gmail.com](mailto:soni44@gmail.com)

Received: November 24, 2022

Accepted: April 19, 2023

Published: April 20, 2023

**Citation:** Kumar S, Soni M, Panthi SK, Ahmed M, Dewang Y. 2023. Analysis the Influence of Various Step Punch Shape and Clearance in Stretch Flanging Process Using FEM Simulation. *NanoWorld J* 9(S1): S390-S396.

**Copyright:** © 2023 Kumar et al. This is an Open Access article distributed under the terms of the Creative Commons Attribution 4.0 International License (CCBY) (<http://creativecommons.org/licenses/by/4.0/>) which permits commercial use, including reproduction, adaptation, and distribution of the article provided the original author and source are credited.

Published by United Scientific Group

## Abstract

Effectiveness of the flanging process depends on geometry of tools, material properties, etc. Punch is an important part of looting and its profile geometry and clearance with respect to die plays the very important role. In this paper, the influence of step punch profiles and gap between the die and the punch were studied using FEM simulation and experiments. FEM simulation of stretch forming process for aluminum alloy AA5052 was carried out using five different punch profiles at 1 mm and 2 mm clearance. Experiments are carried out to validate one case of the punch profile and gap. FEM simulation results were expressed in this way: strain distribution (direction of die profile radius), bending load distribution with displacement of punch, length of cracks, and crack propagation. The peak forming load, radial strain, and circumferential strain were obtained at least gap in every punch case. The edge crack length reduces with increment in clearance between punch and die. The bending load is obtained peak value for the two-step punch shape whereas this value is small for the four-step punch shape. Strain (radial and circumferential strain) attained higher values in two-step punch shape, while these values are the small for four-step punch shape. Therefore, a large number of step punch profiles (more stepped punch) is suitable for mitigation of cracks length in stretch flanging process (SFP).

## Keywords

FEM simulation, Step punch, Stretch flanging process, Strain distribution, Bending load, Edge cracks

## Introduction

Flanging is a more important sheet metal forming process and is one type of bending process. The flanging process has established itself as the most significant sheet metal forming process. It finds its major applications in the production of aircraft and automobile components. The flange portion is used for providing for the smoothness, stiffness, and assemblies of the different parts [1, 2]. Generally, three cases of flanging process are used in the industries they are known as stretch, straight, and shrink flanging. In the realm of stretch flange forming, one end portion of the sheet is bent to 90 degree and form the flange curvature with concave shape [3, 4]. The flange portion is circumferentially stretched in this process along the bend line and cracks occur on the top portion of the flange that is shown in figure 1. In the shrink flanging process, one end side of sheet is bent to 90 degree and form the flange curvature with convex shape. Sheets in the shrink flanging process are circumferentially compressed and wrinkles occur in the lower portion which is shown in figure 2. In stretch flanging, the highest tension occurs

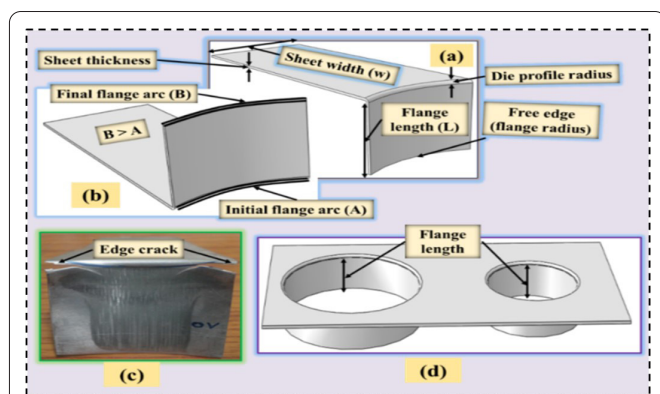


Figure 1: (a, b and c) Non-axisymmetric stretch flanging (without hole flanging) process with cracks and (d) axisymmetric stretch flanging (with hole flanging) process [18, 19].

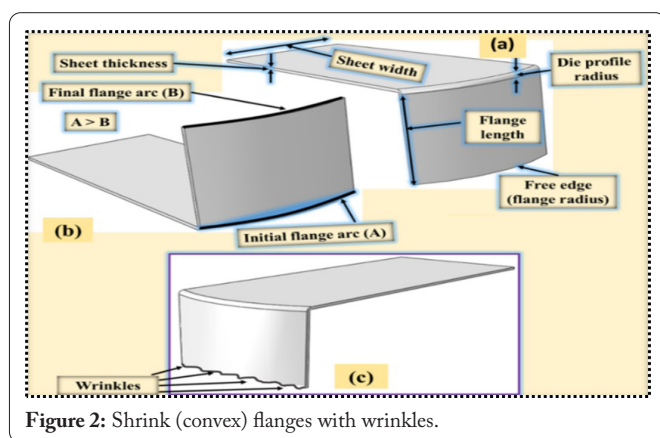


Figure 2: Shrink (convex) flanges with wrinkles.

at the top portion of the flange and maximum hoop strain is the principal deforming parameter. Sheet encounters failure in terms of edge crack due to necking and thinning during stretch flanging. Removal of these kinds of defects is possible by properly designing of tools for the process through FEM modelling and simulation work. The simulation provides a solution which is cost effective and less time consuming than experimental processes.

A lot of researchers have contributed in the past to failure prediction for sheet metal forming. Mathematical model has been developed by Wang and Wenner [5] for prediction of strain-stress distribution in stretch flange forming. The model consists of approximate theory and theory of total strain. In addition to this, Wang et al. [1] also worked for development of analytical model of stretch flanging and predicted the failure and wrinkling criteria in terms of strain. Asnafi [6] studied fracture limit experimentally and theoretically in shrink and stretch flanging by fluid forming process. Hu et al. [7] examined the effect of anisotropic characteristics of material in variety of processes related to sheet forming. Feng et al. [8] studied the effect of geometrical parameters (radius of curvature range, flange height, and curvature radius of punch) in stretch curved flanging and proposed that use of punch with lesser radius than that of die results in ineffective deformation. Dewang et al [9] is one of those who pioneered the SFP using FEM simulation. Wan et al. [10] studied the influence of forming performances in flexible stretch-stamp forming process. Mac et al. [11] predicted the forming limit curve of steel DP350 sheets

by Hecker's punch stretching tests method through FEM simulation and experimental one. Akricchi et al. [12] utilized technique of deep learning for measuring roundness and deviation in position during SPIF. Hu et al. [13] presented mathematical models for contoured flanging process and predicted the profile of rolling-stock and trim-line of blank. Yogesh et al. [14, 15] studied the influence of binding force and thinning and other geometrical parameters in SFP by FEM simulation and experiments also. Li et al. [16] proposed a mathematical model for assessment of present process FSP (V-shaped sheet metal). Kumar et al. [17] predicted length of crack and strain distribution in FSP by FEM simulation. Several authors has been examined the various types of failure criteria/analysis (i.e., fracture, crack, wrinkling, thinning, and ductile failure) in sheet metal forming process (deep drawing and stretch flanging process) [3-23]. Frącz et al. [24] studied the influence of punch geometry in hole flanging process. Many researchers had used the different shape of punches in different sheet metal forming processes for different purpose (mitigation of thinning and cracks, enhanced the formability, and hole expansion limit) [24-28]. It is observed that previous studies pay little attention to the influence of profile radius of punch in SFP.

It is found from literature that very little focus is offered by researchers on influence of punch shape on deformation behaviour of blank in SFP (present process). Deformation of blank depends on type of interaction and surface area interaction between blank and punch in stretch flange forming. In this work, study the influences of step punch profiles and gap between the die and punch on characteristics of deformation in stretch flange forming using aluminum alloy. Experimental and Finite element simulation both are carried for the present work.

## Materials and Methods

### Material

The properties of mechanical of non-annealed aluminum alloy AA5052 was utilized as sheet metal. The material has vast applications for various components in automotive and aerospace applications. Tensile testing of AA5052 sheets was tested as per ASTM E8/E8M-11 on an INSTRON machine equipped with computer and data acquisition system. Figure 3 shows true stress-strain flow curve. Modulus of Elasticity = 70.3 GPa, Poisson's ratio = 0.33, and density = 2680 kg/m<sup>3</sup> were the properties of mechanical of AA5052 sheet metal [17, 19]. The same properties were used in the simulation.

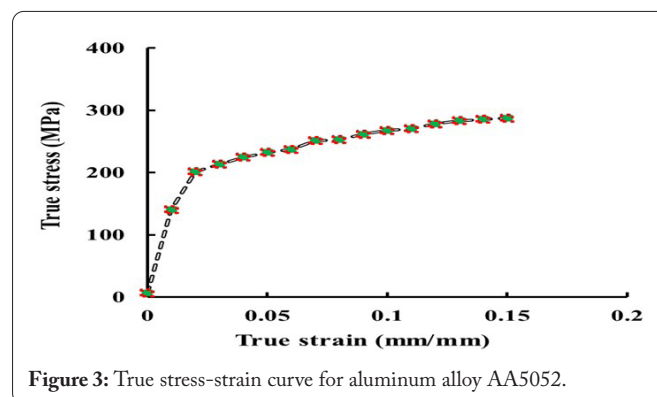


Figure 3: True stress-strain curve for aluminum alloy AA5052.

### FEM modelling and simulation

FEM simulation was carried out for five different cases of stretch flange forming, which were presented clearly in table 1. Figure 4 shows the different step punch profiles considered for the study. FEM model for all cases was developed for estimation of edge crack phenomenon. Figure 5 shows the typical 3D CAD (computer-aided design) and FEM model for the present study. Sheets of dimensions (L x B x H) 120 x 35 x 0.5 mm were utilized for both experiments and FEM simulation. Sheet metal of AA5052 was discretized with C3D8R elements. Four node (R3D4) discrete rigid elements were utilized for meshing of die, binder, and punch. Tool parts are assumed as rigid body and boundary conditions were imposed on reference node of tools. A blank holder was utilized to suppress the sheet over the die and 30 mm of sheet were placed outside free for formation of stretch flange. Die was encastered while punch is made to move in downward vertical direction to form stretch flange. 20 kN of blank holding force is applied and friction coefficient was assumed similar for all cases i.e., 0.1.

Crack initiation in sheet by simulation was investigated by considering shear and ductile modes of damage. By definition of such criteria, mesh will delete automatically which indicates the edge crack phenomenon. Radius of punch and die was considered as 25 mm. Data was collected in terms of strain distribution and requirement of load for forming the flange and edge crack location. Experiments were carried out to validate the result of FEM simulation for one case of punch and sheet.

**Table 1:** Input variables for FEM simulation of SFP.

S. No.	Input variable	Details of variables
1.	Punch profile	Zero step (cylindrical), one step, two step, three step, and four step
2.	Gap between die and punch	1 mm and 2 mm

### Experimental procedure

The blank dimensions (L x B x H) 35 x 120 x 0.5 mm<sup>3</sup> were stretch flange experimentally using zero step punch (cylindrical) of 50 mm diameter with 1 mm and 2 mm gap between die and punch. Hydraulic press with double acting facility was used for performing experiments of stretch flange forming. Overall capacity of Hydraulic press is 50 kN. It comprises a main ram which has a capacity of 30 kN and the other one is the blank ram which is capable of exerting a maximum force of 20 kN. The function of the main ram is to hold the punch tightly and the blank ram is applying is for applying blank holding force during stretch flange forming. Die, punch, blank-holder, and blank were assembled and considered as a tool set-up as shown in figure 6. Similar size of tooling set-up and sheet were realized/applying both in FEM simulation and experiments. The sample positing (fixed and free length of blank) is also similar. Die and punch were fixed/clamped on the worktable and the main ram, respectively. The main ram was moved with velocity of 1 mm/s for formation of stretch flange. After that load was released and blank was taken out. Edge crack position, its propagation and crack length were measured/observed.

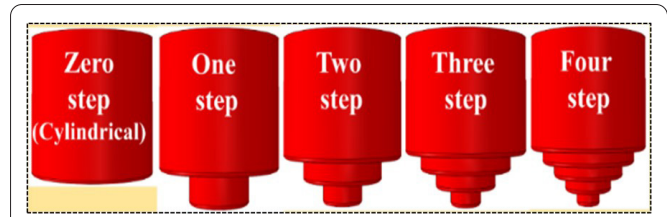


**Figure 4:** Different step punch profiles for FEM analysis of stretch flanging.

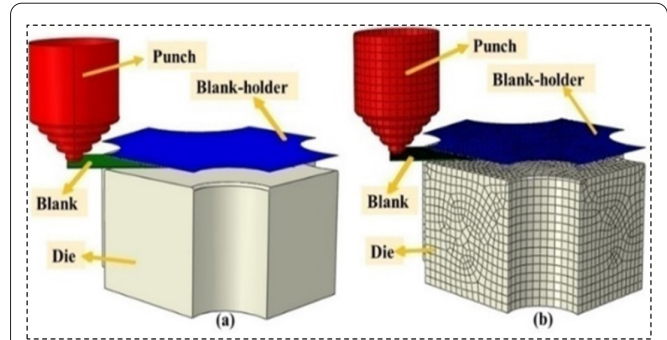


**Figure 5:** Assembled (a) 3D CAD Model and (b) Finite element model of stretch flanging.

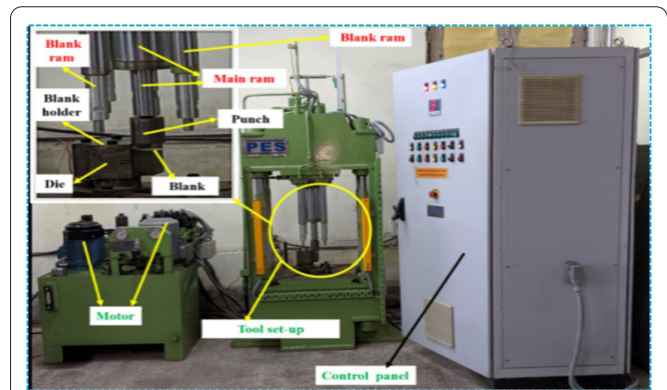


**Figure 6:** 50 kN hydraulic press (double acting) and tool setup for stretch flanging experiments.

### Assessment of peak bending force

This force can be evaluated by applying the following formula [3, 17, 19, 29].

$$\text{Maximum Bending Force (F)} = \left( \frac{K_{bf} * (UTS) * W * t^2}{D} \right) \quad (1)$$

Where,  $K_{bf}$  = Constant (this constant value varying with types of bending operation);  $W$  = sheet width;  $D$  = die opening length;  $t$  = sheet thickness; and  $T_s$  (UTS) = ultimate tensile strength of material. Peak bending load is influenced by the following input variables such as  $D$ ,  $W$ ,  $t$ ,  $UTS$ ,  $K_{bf}$ , friction coefficient between the tool interfaces, tool setup geometry (punch, die, and blank profile). Maximum bending force is illustrated from figure 7 and equation (1) [3, 17, 19, 29].

### Results and Discussion

Present work deals with the study of effect of all punch profiles i.e., zero step, 1 step, 2 step, 3 step, and 4 step punch

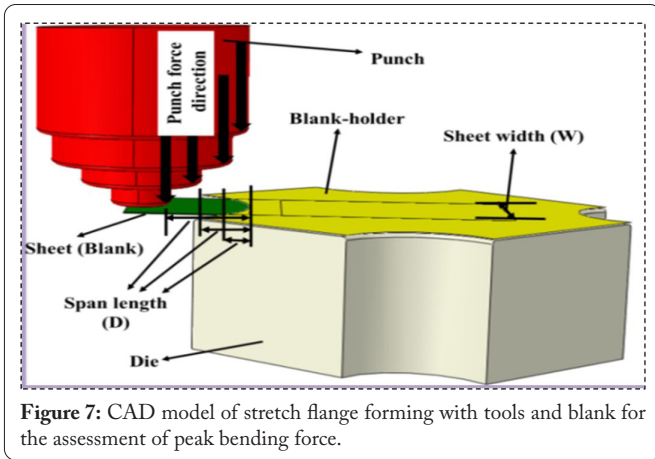


Figure 7: CAD model of stretch flange forming with tools and blank for the assessment of peak bending force.

profile and punch-die gap (1 and 2 mm) were studied in SFP. Considering five types of punch profile and two punch-die clearances, ten cases of stretching flanging arise. In order to confirm the FEM model considered for the study, experiments have been carried out considering only one type of punch (zero step) with both 1 mm and 2 mm punch-die clearance. Validation of finite element simulation results were conducted and expressed in terms of edge crack propagation and its location. Figure 8 shows results of both FEM simulation and experiments for the considered case. As observed the crack starts from edges of the blank and it is located near die corner. It further propagates towards the center of the blank as the punch moves downward. The crack length is measured and listed in table 2 for both cases. Experimental and simulation results vary in the range of 11 - 13% and it is considerable range. The results of finite element simulation were validated with experimental results which are shown in figure 8.

The FEM simulation results of all the cases were ex-

Table 2: Comparison of FEM simulation results with experimental.

S. No.	Condition	Crack length (mm)		Percentage difference
		FEM Simulation	Experimental	
1.	Zero step punch (1 mm gap)	12.5	11.2	11.6 %
2.	Zero step punch (2 mm gap)	8	7.1	12.7 %

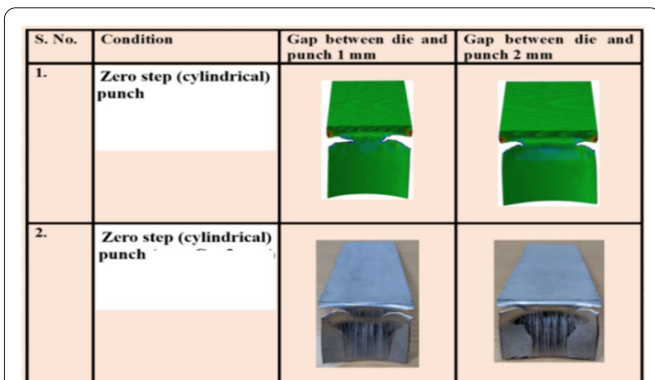


Figure 8: Comparison of deformed flange edge crack position and their propagation in zero step (cylindrical) punch.

pressed in terms of location of edge crack, force requirement for SFP and distribution of strain along free edge of stretch flange. The forming load data was obtained from FEM simulation at selected reference point on punch. Variation of punch force with movement of punch was plotted for different step punch cases at various clearances and given in figure 9. In the cylindrical (zero step) punch profile, forming load increases rapidly as compared to other punch profiles with increment in the punch displacement [9, 14, 15]. It is because of large slope of punch and sudden contact between punch and sheet. Initially punch load increases until the blank bends up to a fixed theta degree and further it decreases because of initiation of crack and its propagation towards the mid-section of the blank. After completion of crack propagation, forming load is almost constant. Slipping of punch over sheet without increase in punch load might be one of the reasons. Punch profile and contact area of tool with blank plays a vital role for forming load distributions. From the figure 9 and figure 10, it is gathered that peak forming punch load is required for two step punch shape. While it is least for the four-step punch shape. It may be due to sudden contact between the sheet and the punch. Therefore, large number of step punch profile (more stepped punch) is suitable for the better deformation in SFP based on the forming load requirement.

Figure 11 shows the contact position of different steps punch through FEM simulation. Punch shape effect the forming load because in these cases span length (die opening length) are varying during the deformation of sheet [3, 17, 29].

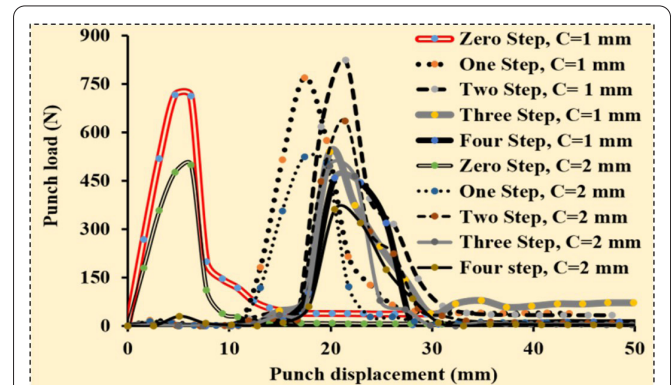


Figure 9: Variation of punch load for different step punch profile and gap between punch and die (C = Clearance/gap) at 25 mm die radius.

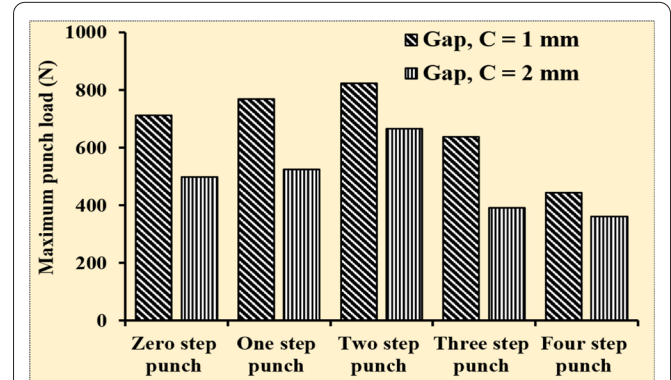
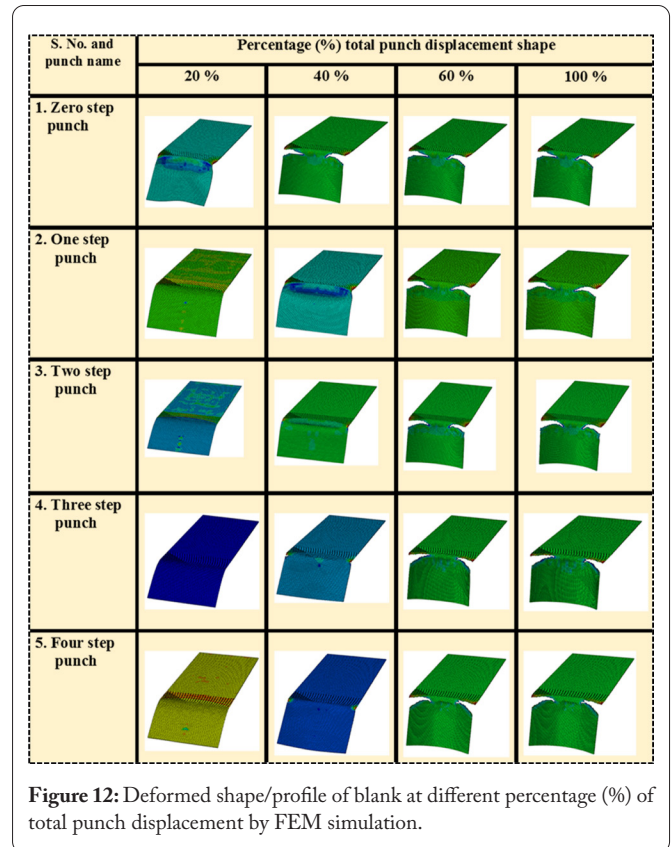
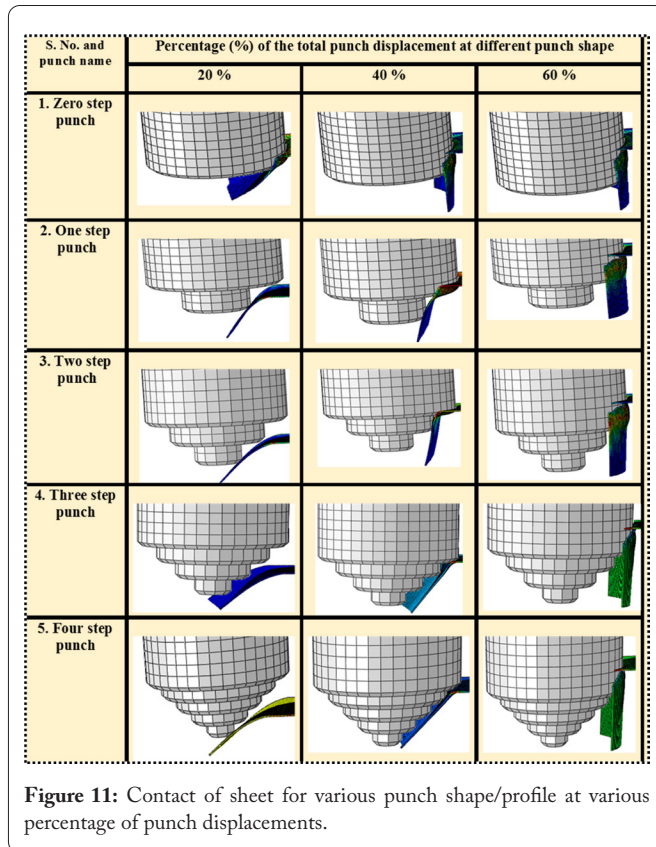


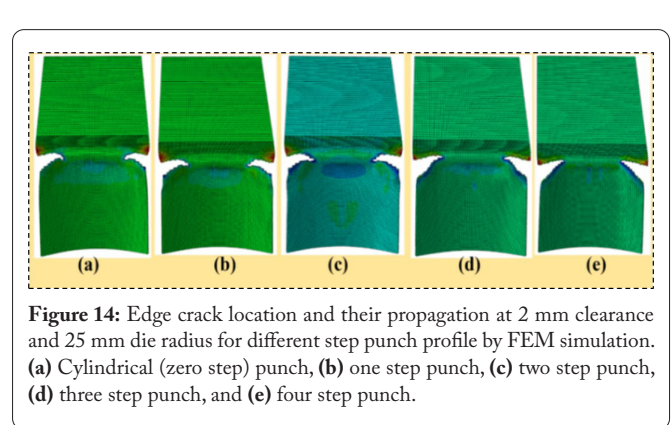
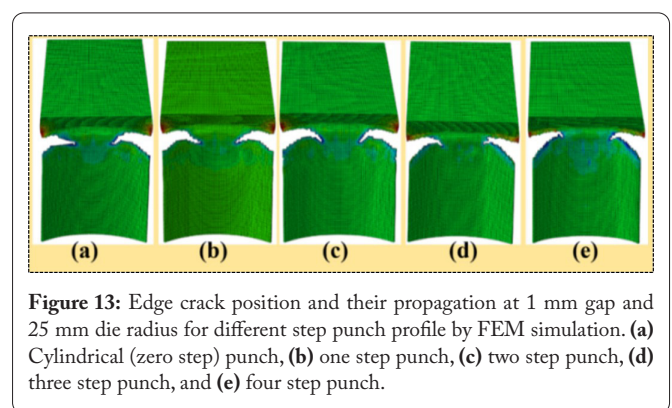
Figure 10: Comparison of maximum punch load for different step punch profile at gap between punch and die C = 1 and 2 by FEM simulation.



Sheet deformation through punch at various displacements of punch i.e., 20, 40, 60, and 100% are shown in figure 12. It is evident from this figure that there is no crack initiation takes place in the blank up to, approximately, 20% of total punch displacement in 1 step, 2 step, 3 step, and 4 step punch, while in case of zero step punch, i.e., cylindrical punch, crack starts at the same percentage of punch displacement. In the case of 1 step, 2 step, 3 step, and 4 step punch crack starts nearly at 40% of total punch displacement whereas significant crack is observed in zero step (cylindrical) punch at the same percentage (40%) of total movement of punch. It is because the large contact between punch and sheet and span length is also small as compared to other step punch (one, two, three, and four step punch) [3, 29]. Hence, different punch shapes illustrate different contact behaviour and deformation of blank during stretch flange forming.

Crack initiation starts from both sides of edge corner of profile radii of die, and it travels towards center of die for all cases. It is understandable from figure 13, figure 14, and figure 15 that crack propagation reduces with increment in die-punch clearance for all cases of punch profiles. Propagation of the crack is found maximum at 1 mm of gap, whereas it is minimum at 2 mm of gap in all step punch profiles.

Distribution of strain along profile radii of die is measured at meridian path. This path was drawn away from the crack position in deformed sheet as shown in figure 16. It is examined that strain are maximum near the edge corner of die profile radius due to maximum stretching of sheet in one direction and maximum compressive in other direction takes place at side corner of die profile radius.



From figure 17 and figure 18, peak strain in circumferential and radial direction found for case of two step punches profile, whereas least strain in circumferential and radial direction are found for four step punch profile.

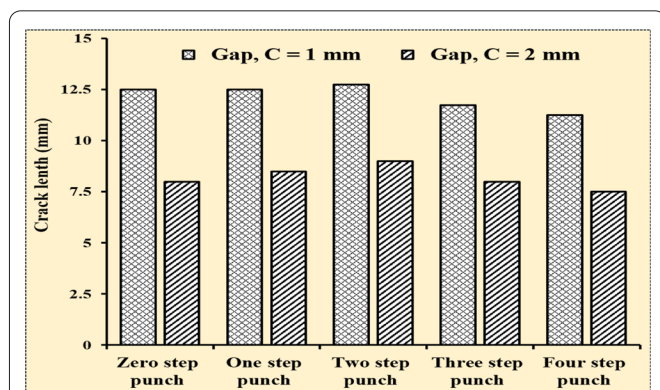


Figure 15: Crack length in blank for different step punch profile at C = 1 and 2 mm by FEM simulation.

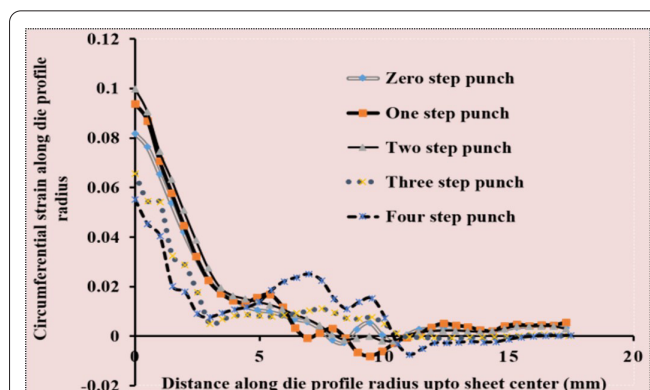


Figure 17: Effect of profile of step punch on circumferential strain at 1 gap between punch and die.

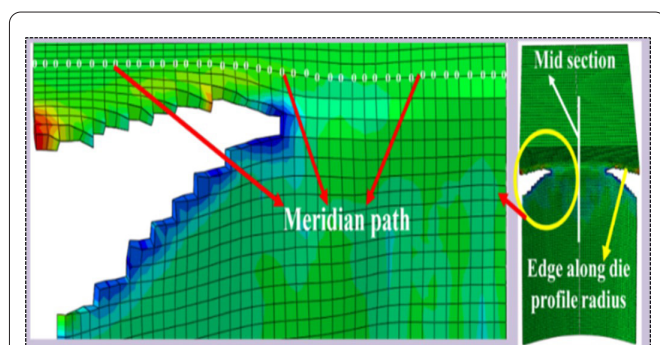


Figure 16: FEM simulation results showing crack propagation and meridian path for analysis of result (strain distribution).

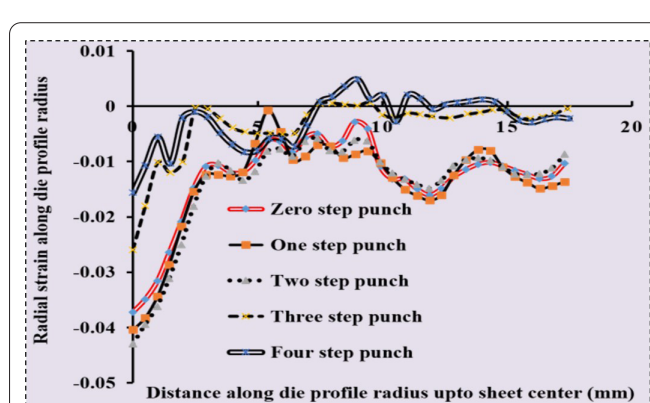


Figure 18: Effect of profile of step punch on radial strain at 1 gap between punch and die.

## Conclusion

In this study, influence of various step punch profiles and gap between die and punch on deformation characteristics of stretch flange forming. FEM simulation mode of SFP has been validated with experiments for one such case. The validation ensures the applicability of FEM model for all the cases considered in the study. Following are the conclusions:

- A minimum forming load is required for four step punch profile in contrast to remaining punch profiles considered in the study.
- Edge crack length increases with decrease in punch die clearance in all step punch profile. Forming loads are also found maximum in 1 mm clearance, whereas it is minimum in 2 mm gap for all types of considered step punch profile.
- Crack initiation in sheet is highly depends on the profile of the punch. It is due to contact behaviour of sheet with punch during deformation.
- Strain in circumferential and radial direction are found to be maximum for two step punch profile, whereas four step punch profile has minimum circumferential as well as radial strain. Therefore, a large number of step punch profile is suitable for better deformation in stretch flanging process. It can be concluded based on the edge crack in sheet, edge crack, strain distribution, and forming load distribution.

## Acknowledgments

The authors would like to thank Director, CSIR-AMPRI, Bhopal, India for providing the facility and support for carrying out the present work.

## Conflict of Interest

The author(s) declared no potential conflicts of interest with respect to the research, authorship, and/or publication of this article.

## Credit Author Statement

Surendra Kumar: Experimentation, Data analysis, Writing - original draft preparation; Manoj Soni: Experimentation, Writing - original draft preparation; S.K. Panthi: Resources, Writing - review and editing; M. Ahmed: Conceptualization, Writing - review and editing; Yogesh Dewang: Experimentation, Writing - review and editing. All the authors read and approved the manuscript.

## References

1. Wang CT, Kinzel G, Altan T. 1995. Failure and wrinkling criteria and mathematical modeling of shrink and stretch flanging operations in sheet-metal forming. *J Mater Process Tech* 53(3-4): 759-780. [https://doi.org/10.1016/0924-0136\(94\)01766-T](https://doi.org/10.1016/0924-0136(94)01766-T)
2. Stachowicz F. 2008. Estimation of hole-flange ability for deep drawing steel sheets. *Arch Civil Mech Eng* 8(2): 167-172. [https://doi.org/10.1016/S1644-9665\(12\)60203-9](https://doi.org/10.1016/S1644-9665(12)60203-9)

3. Kalpakjian S, Schmid SR. 2014. Manufacturing Engineering and Technology. Pearson.
4. Groover MP. 2002. Solutions Manual: Fundamentals of Modern Manufacturing. Wiley.
5. Wang NM, Wenner ML. 1974. An analytical and experimental study of stretch flanging. *Int J Mech Sci* 16(2): 135-143. [https://doi.org/10.1016/0020-7403\(74\)90082-4](https://doi.org/10.1016/0020-7403(74)90082-4)
6. Asnafi N. 1999. On stretch and shrink flanging of sheet aluminium by fluid forming. *J Mater Process Technol* 96(1-3): 198-214. [https://doi.org/10.1016/S0924-0136\(99\)00352-0](https://doi.org/10.1016/S0924-0136(99)00352-0)
7. Hu W, Wang ZR. 2002. Anisotropic characteristics of materials and basic selecting rules with different sheet metal forming processes. *J Mater Process Technol* 127(3): 374-381. [https://doi.org/10.1016/S0924-0136\(02\)00410-7](https://doi.org/10.1016/S0924-0136(02)00410-7)
8. Feng X, Zhongqin L, Shuhui L, Weili X. 2004. Study on the influences of geometrical parameters on the formability of stretch curved flanging by numerical simulation. *J Mater Process Technol* 145(1): 93-98. [https://doi.org/10.1016/S0924-0136\(03\)00866-5](https://doi.org/10.1016/S0924-0136(03)00866-5)
9. Dewang Y, Hora MS, Panthi SK. 2014. Finite element analysis of non-axisymmetric stretch flanging process for prediction of location of failure. *Procedia Mater Sci* 5: 2054-2062. <https://doi.org/10.1016/j.mspro.2014.07.539>
10. Wang Y, Liu DZ, Li R. 2019. Numerical investigation for the flexible stretch-stamp forming process of sheet metal. *Adv Mech Eng* 11(1): 1687814018819287. <https://doi.org/10.1177/1687814018819287>
11. Mac TB, Do VC, Nguyen DT. 2018. A study of combined finite element method simulation/experiment to predict forming limit curves of steel DP350 sheets. *Adv Mech Eng* 10(4): 1687814018768148. <https://doi.org/10.1177/1687814018768148>
12. Akrihi S, Abbassi A, Abid S, Ben Yahia N. 2019. Roundness and positioning deviation prediction in single point incremental forming using deep learning approaches. *Adv Mech Eng* 11(7): 1687814019864465. <https://doi.org/10.1177/1687814019864465>
13. Hu P, Li DY, Li YX. 2003. Analytical models of stretch and shrink flanging. *Int J Mach Tools Manuf* 43(13): 1367-1373. [https://doi.org/10.1016/S0890-6955\(03\)00150-0](https://doi.org/10.1016/S0890-6955(03)00150-0)
14. Dewang Y, Panthi SK, Hora MS. 2019. Binder force effect on stretch flange forming of aluminum alloy. *Mater Manuf Process* 34(13): 1516-1527. <https://doi.org/10.1080/10426914.2019.1655154>
15. Dewang Y, Hora MS, Panthi SK. 2015. Prediction of crack location and propagation in stretch flanging process of aluminum alloy AA-5052 sheet using FEM simulation. *Trans Nonferrous Met Soc China* 25(7): 2308-2320. [https://doi.org/10.1016/S1003-6326\(15\)63846-8](https://doi.org/10.1016/S1003-6326(15)63846-8)
16. Li D, Luo Y, Peng Y, Hu P. 2007. The numerical and analytical study on stretch flanging of V-shaped sheet metal. *J Mater Process Technol* 189(1-3): 262-267. <https://doi.org/10.1016/j.jmatprotec.2007.01.035>
17. Kumar S, Ahmed M, Panthi SK. 2020. Effect of punch profile on deformation behaviour of AA5052 sheet in stretch flanging process. *Arch Civil Mech Eng* 20: 1-17. <https://doi.org/10.1007/s43452-020-00016-2>
18. McDougall JL, Stevenson ME, McKeever K. 2005. Analysis of sheet steel fracture during deep drawing. *J Fail Anal Preven* 5: 20-25. <https://doi.org/10.1361/154770205X65972>
19. Kumar S, Ahmed M, Panthi SK. 2020. Investigation on the crack and thinning behavior of aluminum alloy 5052 sheet in stretch flanging process. *J Fail Anal Preven* 20: 1212-1228. <https://doi.org/10.1007/s11668-020-00922-w>
20. Gupta RK, Anil Kumar V, Karthikeyan MK, Ramkumar P, Ramesh Narayanan P, et al. (2010) Investigation of cracks generated in columbium alloy (C-103) sheets during deep drawing operation. *J Fail Anal Preven* 10: 228-232. <https://doi.org/10.1007/s11668-010-9341-z>
21. Kumar S, Singh P, Soni M, Shakya JP, Panthi SK, et al. 2022. Effects of processes parameters on spring back, wrinkles and cracks in different flanging processes: a review. *IOP Conf Ser Mater Sci Eng* 1259(1): 012014. <https://doi.org/10.1088/1757-899X/1259/1/012014>
22. Kumbhar SV. 2018. Pressure optimization and failure prediction for deep drawing process of sheet metal products: a case study. *J Fail Anal Preven* 18: 948-956. <https://doi.org/10.1007/s11668-018-0485-6>
23. Azodi HD, Safari M, Darabi R. 2017. Formability prediction of two-layer sheets based on ductile fracture criteria. *Trans Indian Inst Met* 70: 1841-1847. <https://doi.org/10.1007/s12666-016-0986-5>
24. Frącz W, Stachowicz F, Trzepieciński T. 2012. Investigations of thickness distribution in hole expanding of thin steel sheets. *Arch Civil Mech Eng* 12: 279-283. <https://doi.org/10.1016/j.acme.2012.06.006>
25. Cao T, Lu B, Ou H, Long H, Chen J. 2016. Investigation on a new hole-flanging approach by incremental sheet forming through a featured tool. *Int J Mach Tools Manuf* 110: 1-17. <https://doi.org/10.1016/j.ijmactools.2016.08.003>
26. Krawczyk J, Gronostajski Z, Polak S, Jaśkiewicz K, Chorzępa W, et al. 2016. The influence of the punch shape and the cutting method on the limit strain in the hole expansion test. *Key Eng Mater* 716: 129-137. <https://doi.org/10.4028/www.scientific.net/KEM.716.129>
27. Kurra S, Regalla SP. 2014. Experimental and numerical studies on formability of extra-deep drawing steel in incremental sheet metal forming. *J Mater Res Technol* 3(2): 158-171. <https://doi.org/10.1016/j.jmrt.2014.03.009>
28. Wen T, Zhang S, Zheng J, Huang Q, Liu Q. 2016. Bi-directional dieless incremental flanging of sheet metals using a bar tool with tapered shoulders. *J Mater Process Technol* 229: 795-803. <https://doi.org/10.1016/j.jmatprotec.2015.11.005>
29. Groover MP. 2020. Fundamentals of Modern Manufacturing: Materials, Processes, and Systems. John Wiley & Sons.